J Mater Sci (2007) 42:2097–2104
DOI 10.1007/s10853-006-0157-x

Role of convective heat removal and electromagnetic field structure in the microwave heating of materials

S. V. Egorov · K. I. Rybakov · V. E. Semenov · Yu. V. Bykov · O. N. Kanygina · E. B. Kulumbaev · V. M. Lelevkin

Received: 5 December 2005 / Accepted: 31 March 2006 / Published online: 18 February 2007

Abstract The temperature distributions arising in a low-loss dielectric sample in the process of microwave heating have been studied by means of numerical simulation. The convective heat removal has been demonstrated to play the determining role in the energy balance of the sample. The obtained temperature distributions have been compared with the results of a purposely designed microwave heating experiment with multi-channel temperature measurement. The temperature on the surface of the sample agreed well to the simulation accounting for convective heat removal. The temperature measured inside the sample was higher than predicted by simulation. The electrodynamic calculations have shown that due to diffraction effects the electromagnetic field inside the sample is inhomogeneous even if the sample is irradiated by microwaves isotropically. Thus, it is concluded that in order to simulate the microwave heating process accurately, it is necessary to account for air convection and calculate the structure of electromagnetic field inside the sample.

S. V. Egorov · K. I. Rybakov (✉) ·
V. E. Semenov · Yu. V. Bykov
Institute of Applied Physics, Russian Academy of Sciences,
46 Ulyanov St., Nizhny Novgorod 603950, Russia
e-mail: rybakov@appl.sci-nnov.ru

O. N. Kanygina · E. B. Kulumbaev · V. M. Lelevkin
Kyrghyz-Russian Slavic University, Bishkek, Kyrghyz Republic

Introduction

High-temperature microwave processing of materials [1–3] is an emerging field of science and technology that attracts a growing interest of researchers worldwide. According to the results of many experimental studies, the use of microwave energy for heating enhances high-temperature processes, such as sintering [4–7], joining [8, 9], annealing [10–12], solid-state chemical reactions [13, 14], etc. In many of these studies the authors have observed reduced process duration, reduced temperature required to carry out processes, compared to the conventional methods not using microwaves for heating, as well as improved microstructure and properties of the final materials.

In developing microwave processing applications, an important role is played by numerical simulation. While repeated experiments aimed on optimizing the microwave heating regimes are time-, labor- and energy-consuming, numerical simulation can be an efficient tool to cut down the costs of application development. However, to be usable for this purpose, a simulation method must possess sufficient accuracy. In particular, solid-state diffusion and other thermally activated processes are highly sensitive to temperature, and it is important to be able to control and simulate the temperature of the material undergoing microwave processing to an accuracy better than 1%.

Most microwave heating processes of technological importance are carried out in cavity applicators whose dimensions are considerably larger than the wavelengths of microwave radiation. These multimode cavities provide better uniformity of the electromagnetic field, which is believed to be extremely important for successful implementation of microwave heating

processes with large-size, complex-shape samples and/or batches of samples [3, 15]. From the simulation viewpoint, multimode structures pose considerable difficulties in the calculation of the electromagnetic field, as compared to single-mode cavity applicators [16, 17]. Many simulations try to avoid these difficulties by assuming that the electromagnetic field and hence the deposited power are distributed uniformly over the volume of the sample. However, in many cases, especially when the samples are not too small in comparison with the microwave wavelength inside the material, the field inside the sample is not uniform even if measures have been taken to equalize the field distribution in an empty cavity applicator.

Another factor that affects the uniformity of temperature is heat removal from the sample. In contrast to conventional furnaces where the heat is delivered to the sample from the outside, in a microwave heating system the heat is generated inside the sample due to dissipation of the microwave energy. The temperature distribution establishes as a result of concurrent heat generation in the volume of the sample and heat removal through the sample surface. Therefore an important role is played by the conditions of heat exchange on the surface. Most simulations use simple boundary conditions for temperature, which assume the heat flux through the surface to be proportional to the temperature difference between the surface of the sample and the cold wall of the applicator, with the proportionality coefficient assumed the same over the entire surface of the sample. However, if the process is conducted in air or other gas environment, the actual heat removal is strongly influenced by convection, and the intensity of heat exchange is pronouncedly non-uniform over the sample surface.

The objective of this paper is to determine the role played by convection and non-uniformity of electromagnetic field in a microwave heating process by comparing calculated and measured temperature distributions.

Experiment

The experiments on multichannel temperature measurement were performed on a 30 GHz/10 kW gyrotron system for microwave processing of materials [18]. The system was developed at the Institute of Applied Physics and used in many experimental studies (see [3] for a review of some of them). The microwave radiation from the gyrotron is fed into the applicator, which comprises a cylindrical supermultimode cavity. Hundreds of modes excited simultaneously in the cavity are additionally stirred by a rotating mode stirrer, in order to obtain a more uniform distribution of the electromagnetic field.

A cylindrical alumina ceramic sample was positioned in the cavity on a support made of porous quartz. The dimensions of the cavity, sample and support are shown in Fig. 1. Although in the majority of experiments the sample undergoing the processing is surrounded by thermal insulation, in this particular experiment no thermal insulation was used, to facilitate the comparison with simulation described below. The temperature was measured at eight points of the sample by type K thermocouples, positioned as shown in Fig. 2.

The gyrotron system is equipped with a feedback-loop power control circuit for automatic control over the gyrotron output power in accordance with a preset temperature-time schedule. The reading from one of the temperature sensors is compared with the scheduled temperature, and the power is increased or decreased depending on the difference. The accuracy of sustaining the preset temperature-time schedule in the system is about 1%. In the described experiments, a constant heating rate, 20 K/min, was preset, and the reading from the thermocouple # 8 (positioned in the upper region of the side surface, Fig. 2) was used in the feedback loop of the power control circuit. An example

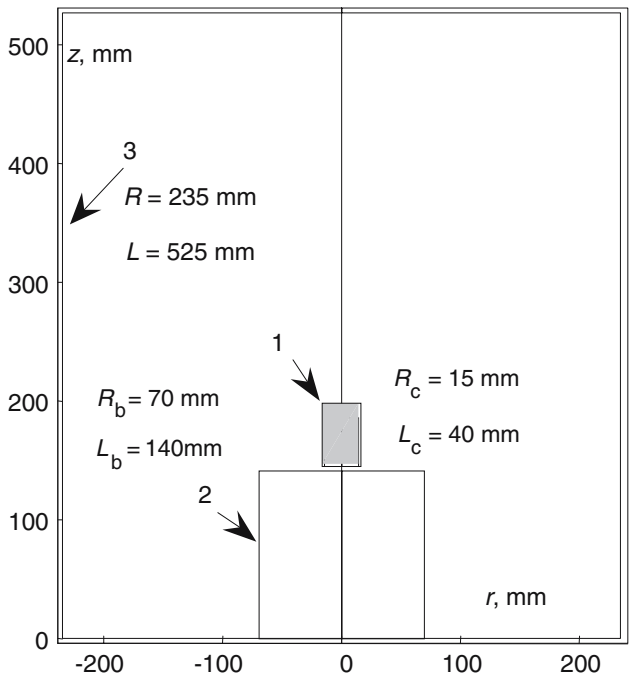

Fig. 1 Dimensions of the ceramic sample (1) on the support (2) in the supermultimode cavity applicator (3) of the gyrotron system

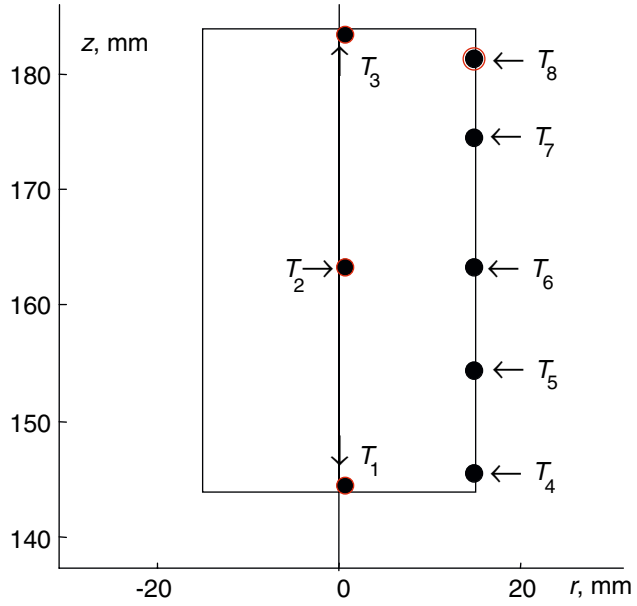

Fig. 2 Positions of the thermocouple sensors of the multichannel system for temperature measurements

of the recorded temperature signal and the gyrotron output power in one of the microwave heating processes is shown in Fig. 3.

The properties of the materials of the sample and support have been determined by separate experiments. The material of the sample is 94 % dense sintered pure alumina (Al_2O_3, ρ = 3.73 g/cm^3). Its specific heat capacity and thermal conductivity were measured on the sample by a standard dynamic calorimetric method. The results of measurements are listed in Table 1 for a range of temperatures. The complex dielectric permittivity of the material was determined by a cavity perturbation technique; its representative value at T = 400 °C which is used in the calculation of the electromagnetic field distribution is $\varepsilon = 9.5 + i\ 0.01$.

The support is made of microwave-transparent porous needle-structured quartz (T3MK-10) with a density of ρ = 0.144 g/cm^3. Its specific heat capacity, C = 947 J/kg K, was calculated based on the reference data for dense quartz. The thermal conductivity was determined from the measurements of steady-state temperature distributions on a cylindrical sample of the material heated from its axis. The thermal conductivity values obtained from these measurements are listed in Table 2.

Model

The evolution of the temperature distribution is described by a model that accounts for volumetric microwave heating of the sample and its cooling by conductive and convective heat transfer into the surrounding air (the radiation heat losses are negligibly small since the temperatures do not exceed 400 °C). As a rough approximation, the power deposition due to microwave heating is assumed to be uniform within the

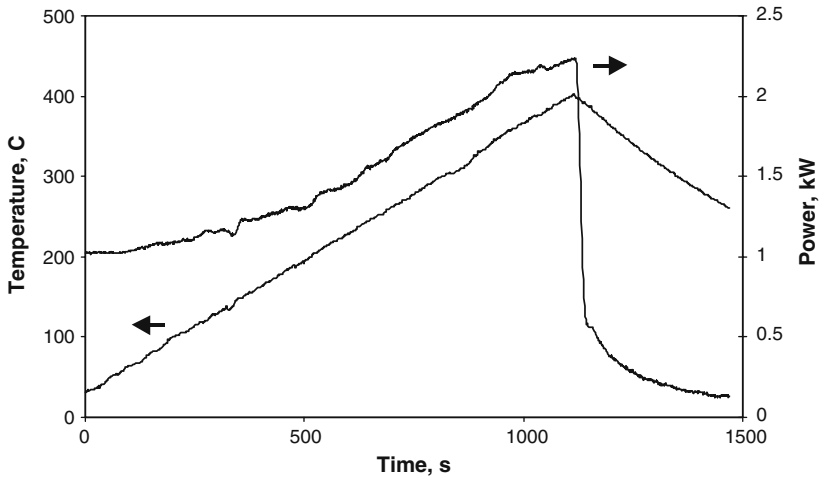

Fig. 3 Temperature and gyrotron output power recorded during a microwave heating process

Table 1 Specific heat capacity and thermal conductivity of alumina, ρ = 3.73 g/cm^3

T, °C	0	50	100	150	200	250	300	350	400
C, J/kg·K	704	799	921	979	996	1003	1065	1062	1068
λ, W/m·K	8.83	8.05	6.52	5.8	5.49	5.3	5.17	4.49	4.07

Table 2 Thermal conductivity of the T3MK-10 material

T, °C	20	33	340	650
λ, W/m·K	0.06	0.08	0.1	0.21

volume of the sample. The limitations of this approximation are discussed below in the Discussion section.

The heating process is described by the equations of continuity, Navier–Stokes, and energy balance. In cylindrical coordinates (see Fig. 1) for the axially symmetric case the equations take the following form:

$$\frac{\partial \rho}{\partial t}+\frac{1}{r}\frac{\partial}{\partial r}(r\rho v)+\frac{\partial}{\partial z}(\rho u)=0;$$

$$\rho\left(\frac{\partial v}{\partial t}+v\frac{\partial v}{\partial r}+u\frac{\partial v}{\partial r}\right)=-\frac{\partial p}{\partial r}+\frac{2}{r}\frac{\partial}{\partial r}\left(r\eta\frac{\partial v}{\partial r}\right)-\frac{2\eta v}{r^2}+\frac{\partial}{\partial z}\left[\eta\left(\frac{\partial u}{\partial r}+\frac{\partial v}{\partial z}\right)\right]-\frac{\partial}{\partial r}\left[\frac{2}{3}\eta\left(\frac{1}{r}\frac{\partial rv}{\partial r}+\frac{\partial u}{\partial z}\right)\right];$$

$$\rho\left(\frac{\partial u}{\partial t}+v\frac{\partial u}{\partial r}+u\frac{\partial u}{\partial z}\right)=-\frac{\partial p}{\partial z}+2\frac{\partial}{\partial z}\left(\eta\frac{\partial u}{\partial z}\right)+\frac{1}{r}\frac{\partial}{\partial r}\left[r\eta\left(\frac{\partial u}{\partial r}+\frac{\partial v}{\partial z}\right)\right]-\frac{\partial}{\partial z}\left[\frac{2}{3}\eta\left(\frac{1}{r}\frac{\partial rv}{\partial r}+\frac{\partial u}{\partial z}\right)\right]+(\rho_\infty-\rho)g;$$

$$\rho C\left(\frac{\partial T}{\partial t}+u\frac{\partial T}{\partial z}+v\frac{\partial T}{\partial r}\right)=\frac{1}{r}\frac{\partial}{\partial r}\left(r\lambda\frac{\partial T}{\partial r}\right)+\frac{\partial}{\partial z}\left(\lambda\frac{\partial T}{\partial z}\right)+P(t).$$

Here $\vec{V}=(V_r=v,\ V_\varphi=0,\ V_z=u)$ is velocity of air, T is temperature, p is pressure, g is free fall acceleration, ρ, λ, C, η are density, thermal conductivity, heat capacity and viscosity, respectively, ρ_∞ is density of ''cold'' air. $P(t)$ is the heat source term that expresses microwave power deposition.

The boundary conditions are defined on the rectangular contour of the simulation area, $0\le r\le R, 0\le z\le L$ (Fig. 1). They include axial symmetry, fixed temperature and zero velocity of air at the cavity walls:

$$0\le z\le L;\quad r=0:\quad \frac{\partial T}{\partial r}=0;\quad \frac{\partial u}{\partial r}=0;\quad v=0;$$
$$r=R:\quad T=T_R;\quad u=v=0;$$

$$0\le r\le R;\ z=0;\ L:\quad T=T_R;\ u=v=0.$$

The microwave-induced heat source is the primary cause of temperature evolution in the system. However, in order to accomplish proper comparison with experiment, where the microwave power is controlled to implement a preset temperature-time schedule, an inverse problem is solved in this simulation. A certain temperature-time schedule is given for one point of the sample, and the temperature evolution in all other points of the simulation volume, as well as the time dependence of the microwave power, $P(t)$, are obtained.

The computation method is based on a through calculation, in which conjugation of problems in the solid bodies and in the air is achieved by introducing harmonic-average transport coefficients on the boundaries between them [19]; inside the solid bodies the viscosity values are taken high enough to ensure zero velocities. The equations are digitized using the control volume method. The pressure field is computed by the SIMPLER procedure [19]. The microwave power, $P(t)$, at any given moment of time is obtained from the energy balance equation at the point of the sample for which the temperature-time schedule is prescribed.

Results and discussion

An example of the simulation results is shown in Fig. 4. The temperature-time schedule of the upper point of the side surface of the sample, $T_8(t)$, was chosen as $T_8=T_R+\alpha t$, where the heating rate, α, was chosen equal to 20 K/min in accordance with experiment.

As the sample is heated due to dissipation of the energy of the microwave electromagnetic field, the air surrounding the sample also heats up and its density decreases. Gradients of air density form within the applicator and they cause convective air flows. Hot air goes up, transports heat to the applicator walls, cools down and descends along the walls. As a result, a gas flow with a non-uniform temperature distribution is established in the applicator (Fig. 4, a–c). For comparison, the case of conductive heat transport only (no convection) is illustrated by Fig. 4d. The temperature inside the sample is also non-uniform (Fig. 5), with a maximum temperature difference between the core and the surface of the sample about 20 K for the chosen heating rate.

Figure 6 shows the time dependencies of the microwave power, $P(t)$, normalized by its maximum value. The microwave power has been computed for three cases: with an account for both convective and conductive heat removal from the sample (curve 1), conductive heat removal only, no convection (curve 2), and no heat removal from the sample (curve 3). For comparison, the microwave power recorded in a microwave heating experiment with constant heating rate (cf. Fig. 3) is

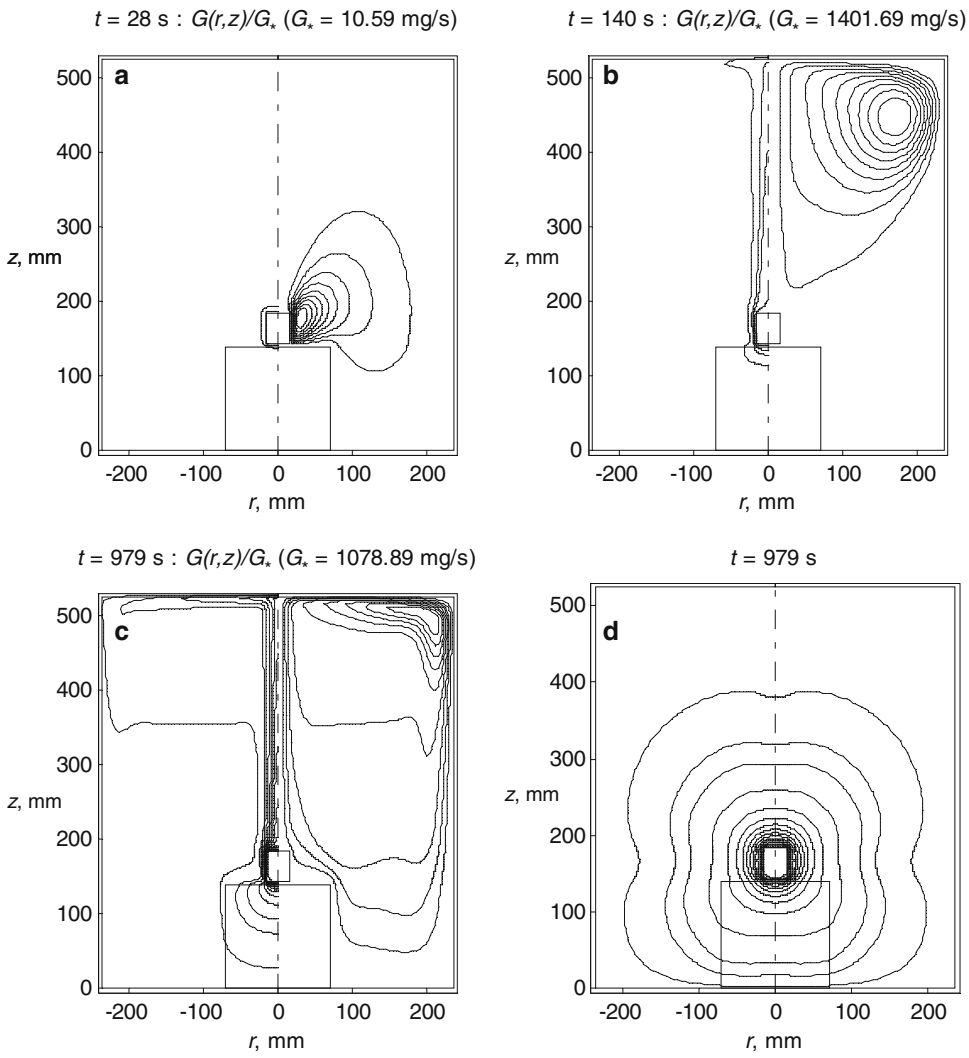

Fig. 4 Calculated dynamics of microwave heating with an account for convective and conductive heat transport: (**a**) at t = 28 s, (**b**) at t = 140 s, (**c**) at t = 979 s. Left: the temperature field (isotherms 301 K, 305 K, 310 K, 325 K and so on with a step of 25 K); right: gas flow lines (from 0.1 with a step of 0.1). (**d**) the case of conductive heat transport only (no convection, isotherms only). The heating rate is 20 K/min.

$$G(r,z) = \int_0^r \rho(r',z)u(r',z)2\pi r'\mathrm{d}r'$$

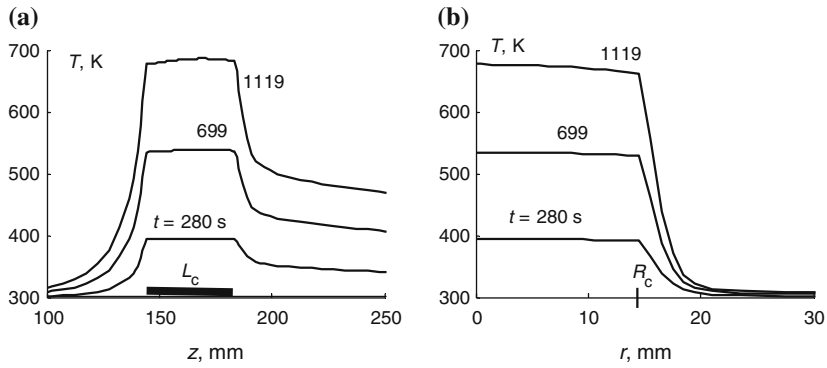

Fig. 5 Distributions of temperature in the applicator containing the ceramic sample: (**a**) in the axial direction, (**b**) in the radial direction (in the middle section of the ceramic sample). The heating rate is 20 K/min

shown (curve 4). It can be seen that the simulation result that accounts for convective and conductive heat removal is, on the average, the closest to the experimental curve. By comparing curves 1, 2 and 3 it can be seen that convective heat removal is prevailing over conductive during the entire process, except its initial stage, when the temperature difference between the sample and the applicator walls is insignificant. At higher temperatures the convective heat removal is about 4 times stronger than conductive.

Figure 7 shows comparison of the calculated and measured temperatures at eight points of the sample. It can be seen that while the measured temperatures on the side surface of the sample agree well with the

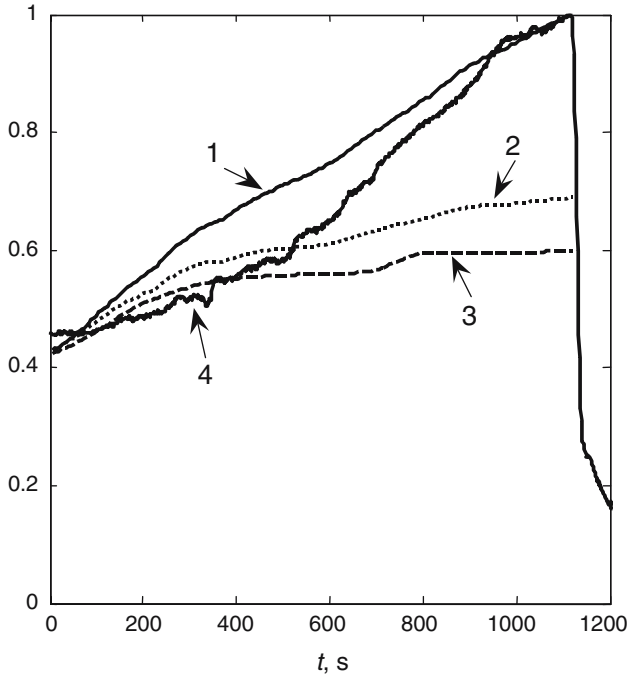

Fig. 6 Time dependencies of the microwave power, $P(t)$, normalized by its maximum value. (1) calculated with an account for both convective and conductive heat removal from the sample, (2) calculated with conductive heat removal only (no convection), (3) calculated with no heat removal from the sample, (4) experimental curve from a microwave heating experiment with the same heating rate (20 K/min)

simulation (taking both convective and conductive heat removal into account), the measured temperatures on the axis of the sample (T_1, T_3) and especially in its core (T_2) are noticeably higher than those predicted by simulation.

To explain this discrepancy, we should recognize that the actual distribution of the deposited power over the volume of the sample is not uniform, as assumed in the simulation described above. The fact that the temperature in the core is higher than predicted by the simulation that assumes uniform electromagnetic field distribution suggests that the field is concentrated in the core region of the sample.

In the microwave heating practice with high-loss materials (such as food in domestic microwave ovens) the field is commonly attenuated from the surface of the sample to the bulk due to the so-called skin effect. However, in certain cases when the dielectric loss tangent of the material is low, the field may form resonant structures inside the sample, sometimes with significant concentration of the field in a small part of the sample [20].

To assess the extent of non-uniformity of the electromagnetic field in the described experiments, the electromagnetic field distribution was calculated

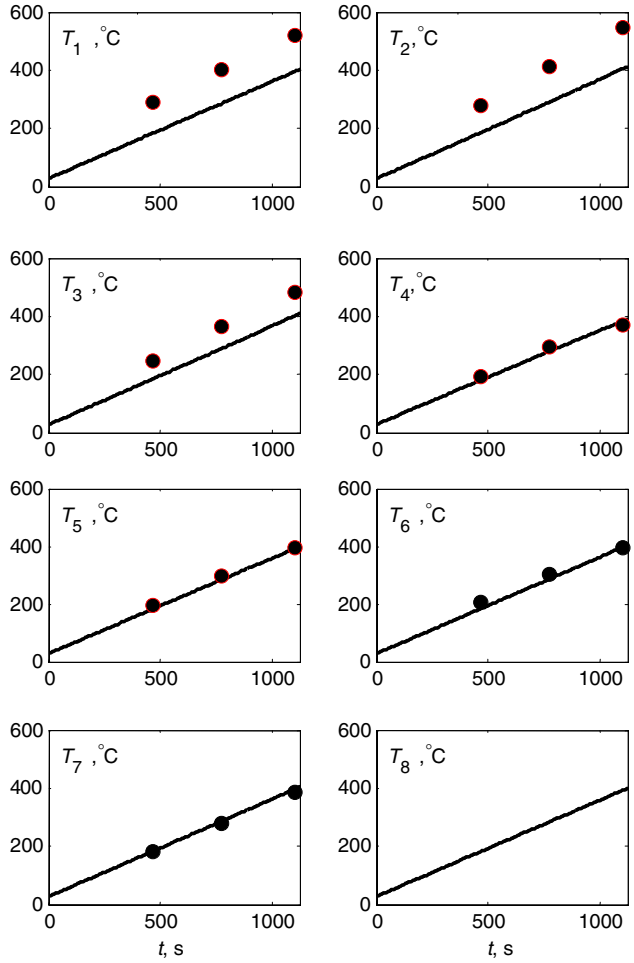

Fig. 7 Temperature of different points of the sample (solid lines—simulated, dots—measured). The temperature-time schedule $T_8(t)$ was preset as a constant heating rate, 20 K/min. See Fig. 2 for positions of the points

for an infinite dielectric cylinder irradiated by a plane electromagnetic wave in which the electric field vector is parallel to the cylinder axis. The electric field inside the cylinder is [21]

$$E_z(r,\varphi) = E_0 \sum_{n=-\infty}^{\infty} A_n J_n\left(kr\sqrt{\varepsilon}\right) e^{\mathrm{i}n\varphi},$$

where

$$A_n = i^n J_n(ka)\left\{1 - \frac{1}{J_n(ka\sqrt{\varepsilon})}\left[\frac{\frac{\varepsilon J_n'(ka\sqrt{\varepsilon})}{ka\sqrt{\varepsilon}J_n(ka\sqrt{\varepsilon})} - \frac{J_n'(ka)}{kaJ_n(ka)}}{\frac{\varepsilon J_n'(ka\sqrt{\varepsilon})}{ka\sqrt{\varepsilon}J_n(ka\sqrt{\varepsilon})} - \frac{H_n^{(2)\prime}(ka)}{kaH_n^{(2)}(ka)}}\right]\right\},$$

J and $H^{(2)}$ are Bessel functions and Hankel functions of the second kind, respectively, E_0 is the amplitude of electric field in the incident wave, $k = \omega/c$ is the vacuum wavenumber, ε is dielectric permittivity of the

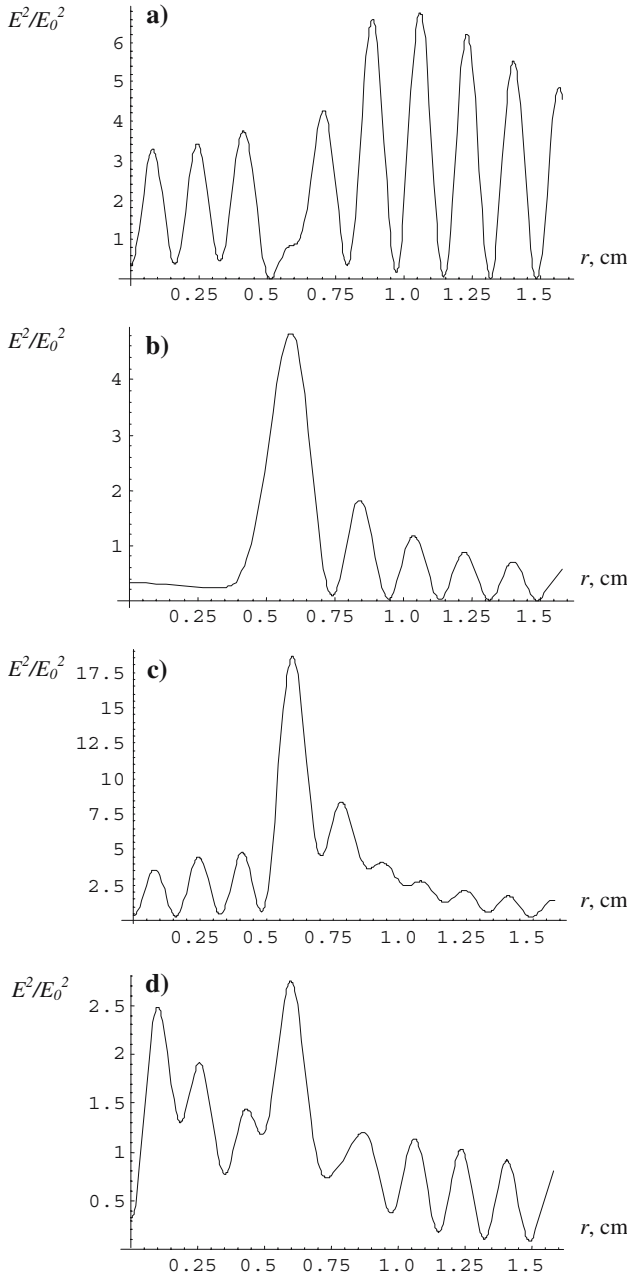

Fig. 8 The square of electric field versus radial coordinate, r, of the cylindrical sample of radius $a = 1.58$ cm made of alumina with the dielectric permittivity $\varepsilon = 9.5 + i\,0.01$ irradiated by a plane electromagnetic wave of frequency 30 GHz in which the electric field vector is parallel to the cylinder axis. (**a**) $\varphi = 0$, (**b**) $\varphi = \pi/2$, (**c**) $\varphi = \pi$, (**d**) averaged over φ. E_0 is the electric field amplitude in the incident wave

material, a is radius of the cylinder. The calculated distributions of the square of electric field in a cylinder with the radius and dielectric permittivity corresponding to the sample used in the experiments are shown in Fig. 8. In particular, the distribution in Fig. 8d, is obtained by averaging over the polar angle, φ, which reflects the fact that in the actual applicator the sample is irradiated by electromagnetic waves uniformly from all directions. It can be seen that the field and hence the distribution of the deposited microwave power are highly non-uniform and exhibit localized areas of field concentration.

Conclusions

A comparative experimental and numerical study of the process of microwave heating of a low-loss dielectric sample in air in a supermultimode cavity applicator has been accomplished. It has been shown that convective heat removal prevails over thermal conduction of air, starting from early stages of the process. The simulation taking convection into account results in a good agreement of the measured and calculated values of temperature on the surface of the sample. However, the measured temperature in the bulk of the sample is higher than predicted by simulation. This is associated with the non-uniformity of electromagnetic field inside the sample, which was not accounted for in the simulation. The distribution of electric field in a dielectric cylinder has been shown to be highly non-uniform, with localized areas of resonant field concentration.

The results of this research demonstrate that commonly used simple models are inadequate for correct simulation of microwave heating processes. Accurate simulation should take into account the heat removal by convective air flows and the distribution of electromagnetic field in the sample. Both of these tasks involve considerable technical difficulties. In particular, they require detailed knowledge of temperature-dependent material properties and significant computer resources. However, accurate process modeling is a necessary step to implement really intelligent microwave processing of materials.

References

1. Clark DE, Sutton WH, Lewis DA (1996) Annu Rev Mater Sci 26:299
2. Thostenson ET, Chou T-W (1999) Composites A 30:1055
3. Bykov YuV, Rybakov KI, Semenov VE (2001) J Physics D: Applied Physics 34:R55
4. Sutton WH (1992) Mater Res Soc Symp Proc 269:3
5. Rödiger K et al (1998) Int J Refractory Metals Hard Mater 16:409
6. Roy R et al (1999) Nature 399:668
7. Sano S et al (2000) J Mater Sci Lett 19:2247
8. Siores E, Do Rego D (1995) J Mater Proc Technol 48:619
9. Lewis D et al (2004) Sci Tech Weld Join 9:459
10. Xu L et al (1997) J Mater Sci Lett 16:1249
11. Bykov YuV et al (2001) J Mater Sci 36:131

12. Thompson K et al (2001) In: Proceedings of the 9th International Conference on Advanced Thermal Processing of Semiconductors—RTP 2001. IEEE Publications, New York, p 190
13. Thomas JJ et al (1996) J Am Ceram Soc 79:2458
14. Vaidhyanathan B et al (2001) J Am Ceram Soc 84:1197
15. Saji T (1996) Mater Res Soc Symp Proc 430:15
16. Dibben DC, Fu WB, Metaxas RAC (1994) Mater Res Soc Symp Proc 347:305
17. Iskander MF et al (1994) IEEE Trans Microwave Theory Tech 42:793
18. Bykov Yu et al (1995) Ceramic Trans 59:133
19. Patankar SV (1980) Numerical heat transfer and fluid flow: computational methods in mechanics and thermal science. Hemisphere Publishing Corporation, New York
20. Rybakov KI et al (2006) J Appl Phys 99:023506
21. Wait JR (1959) Electromagnetic radiation from cylindrical structures. Pergamon Press, London